JOURNAL OF COMPUTATIONAL PHYSICS **125,** 325–337 (1996)
ARTICLE NO. 0097

# Biological Applications of the Dynamics of Twisted Elastic Rods

I. KLAPPER

*Department of Mathematics, University of California, Los Angeles, California 90024*

Received November 28, 1994; revised September 11, 1995

A numerical algorithm for the three-dimensional dynamical viscous Kirchhoff rod model is presented. The algorithm includes proscribed extension and contact forces. Numerical results for several problems of biological significance are given, including dynamics of the writhing (or supercoiling) instability in closed rods and the approach to stable equilibria, and the dynamics and instability of open rods, particularly with regards to the self-assembly behavior of fibril structures composed of the bacteria *bacillus subtilis.* 

## 1. INTRODUCTION

The study of elastic rods has a long history and is the subject of continued scientific and mathematical interest. A rod is defined to be a structure with length much greater than diameter, where for the purposes of this paper it will be assumed that the cross section is circular of constant radius $a$. Applications of the dynamics of rods and filaments range from integrable PDEs [1–3] to DNA conformation [4–7] to three-dimensional scroll waves [8, 9] to the writhing of telephone cable [10] to the formation of sunspots and the heating of the solar corona [11, 12], etc. While the static theory of elastic rods is classical and well studied, their dynamics have only recently received attention and issues arise particularly with regards to computational methods. This paper addresses some of these issues and presents results obtained using a computational model of a linear viscoelastic rod subjected to nonequilibrium forcing. The immediate aim is to present a practical working algorithm for the dynamical Kirchhoff rod model in the context of several specific biological applications.

The original classical work on the theory of rods under linear elastic forces is due to Kirchhoff [13], Clebsch [14], and Love [15]. A short overview of this theory will be presented in Section 2. Most work on the Kirchhoff model to date has concentrated on questions of static equilibrium (see, for instance, [16, Chap. 2]). More recently, consideration has been given to elastic rod dynamics, especially in two dimensions and with regards to the classification of travelling waves (e.g., [17, 18]). In the case of three-dimensional rods, Simo and Vu-Quoc [19] have presented an algorithm for shearable, extensible elastic rods. Here we describe an algorithm for the study of inextensible elastic rods in three dimensions. Related work is being done concurrently elsewhere [20]. In Sections 3, 4, and 5 an algorithm for the dynamics of an inextensible twisted filament will be developed. The principle points to be considered are the tracking of twist evolution and enforcement of inextensibility. Enforced inextensibility is then generalized to proscribed extensibility. One phenomenon that can be explored using this algorithm is the ''writhing'' or ''supercoiling'' instability observed in twisted elastic filaments. The energetics of the circular, uniformly twisted equilibrium configuration were analyzed by Zajac [10] (and again independently by Benham [5]) indicating that for a certain critical total twist this configuration no longer has minimum energy. In Section 6 illustrations of the dynamics of the instability and the evolution of twist and writhe are presented. We also consider the approach to stable equilibrium with contact forces and note the possibility for more than one dynamically attainable equilibrium conformation starting from similar initial conditions. In Section 7 instabilities in the dynamics of open filaments are considered. Open elastic filaments arise, for example, in the context of the macro-fibers formed by chains of the bacteria *bacillus subtilis.* Growing and twisting chains of these bacteria cells become unstable and exhibit complicated writhing behavior [21]. Instabilities in open filaments can *only* be effectively studied dynamically. Current energy minimization methods fail because they assume constant (and hence, in the case of open filaments with circular cross section, zero) twist. Behavior of the dynamical open rod suggests a straightforward explanation for the behavior of filaments of the bacterial *bacillus subtilis.*

## 2. THE KIRCHHOFF ROD MODEL

One can certainly model an elastic filament using the three-dimensional equations of elasticity theory. However, under some circumstances it is to be expected that such a filament can be well-described as a one-dimensional system of equations. One set of such equations, the Kirchhoff rod equations, can be constructed as follows. (For a detailed discussion of the Kirchhoff rod equations and their underlying assumptions, see [23].) The rod is represented by a



0021-9991/96 $18.00

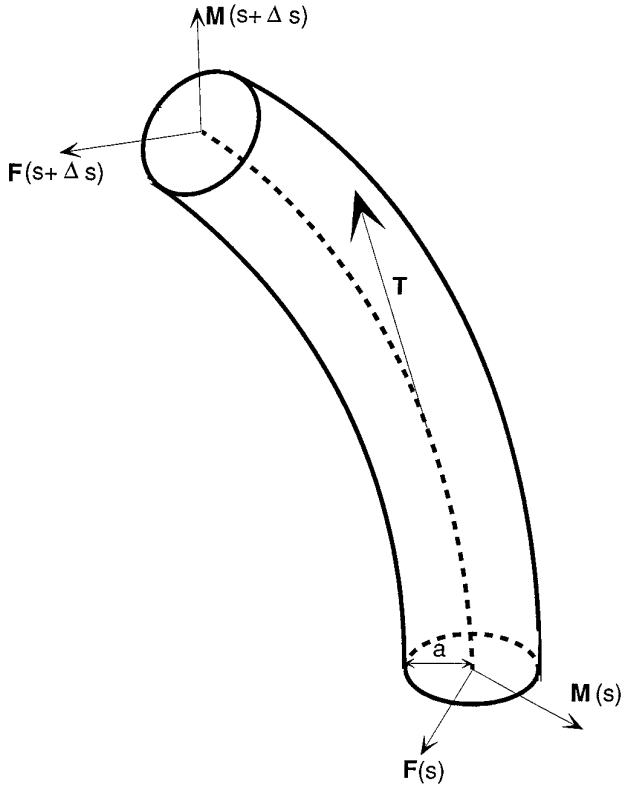


**FIG. 1.** The balance of forces and torques on a short segment of the Kirchhoff rod.

space curve $\mathbf{X}(s, t) : [0, L] \to R^3$ and twist (to be defined below) $\omega(s, t) : [0, L] \to R$ (it is assumed that everything is as smooth as needed throughout). Here $s$ is arclength and $L$ is the total length of the rod. For simplicity it is assumed that the rod has circular cross section with constant radius in both time and space. It will also be assumed that a material cross section perpendicular in the relaxed state remains perpendicular for all time (unshearability). In the case of a closed filament, $\mathbf{X}(0, t) = \mathbf{X}(L, t)$ and $\omega(0, t) = \omega(L, t)$. The unit tangent vector along the curve $\mathbf{X}$ is given by $\mathbf{T}(s, t) = (d/ds)\mathbf{X}(s, t)$. Define a reference ribbon by a pair of curves $(\mathbf{X}, \mathbf{X} + a\mathbf{V})$, where $\mathbf{V}(s, t) : [0, L] \to R^3$ is a unit vector field such that $\mathbf{V} \cdot \mathbf{T} = 0$ and $a$ is the radius of the filament cross section. The twist $\omega$ (with respect to the reference ribbon $(\mathbf{X}, \mathbf{X} + \mathbf{V})$) is defined to be the rotation rate of $\mathbf{V}$ around $\mathbf{T}$ moving along $\mathbf{X}$; i.e., $\omega(s, t) = (\mathbf{V}(s, t) \times (d/ds)\mathbf{V}(s, t)) \cdot \mathbf{T}$. The choice of $\mathbf{V}$ is fairly arbitrary; it will be assumed that $\mathbf{V}$ is a smooth material vector field chosen such that $\omega = \omega_0$, the relaxed twist, when the rod is in an energetically relaxed conformation. With this requirement satisfied, $\omega$ is independent of the choice of the ribbon's initial condition and, under the uniform isotropy assumption made above, the twist can be identified with the torsional strain of the rod. For non-isotropic rods, choosing the reference ribbon to lie in the direction of one of the principle bending directions may be more convenient. Of course, for more general cross sections the relation between twist and torsional strain may not be as simple (although it still exists).

The Kirchhoff model divides the rod into short (relative to all length scales present other than the filament radius) segments (Fig. 1) and balances the local forces and torques (see, e.g., [16]). Define $\mathbf{F}(s, t)$ to be the averaged (or resultant) internal stress on the perpendicular cross section at $\mathbf{X}(s, t)$. Then balancing the internal resultants $\mathbf{F}(s + \Delta s, t) - \mathbf{F}(s, t) \approx (d/ds)\mathbf{F}(s, t)\Delta s$ with the "external" forces gives

$$\rho\pi a^2 \frac{d^2}{dt^2}\mathbf{X} = \frac{d}{ds}\mathbf{F} - \gamma_1 \frac{d}{dt}\mathbf{X} + \mathbf{g}, \tag{1}$$

where $\rho$ is the filament mass density, $-\gamma_1\dot{\mathbf{X}}$ is the viscous drag force, and $\mathbf{g}(s, t)$ contains the other true external forces such as gravity, contact forces, etc. A similar equation can be derived using balance of torques as follows. Define $\mathbf{M}(s, t)$ to be the resultant internal moment on the perpendicular cross section at $\mathbf{X}(s, t)$. The moment on the cross section at $\mathbf{X}(s, t)$ must be balanced by the moment on the cross section at $\mathbf{X}(s + \Delta s, t)$, the induced internal moment $-\Delta s\mathbf{T} \times \mathbf{F}(s, t)$, plus any "external" moments. The resulting equation, which includes a representation of angular inertia and damping in a form which distinguishes contributions of tangential and cross-sectional components, can then be written as

$$\frac{d}{ds}\mathbf{M} = \mathbf{F} \times \mathbf{T} + \rho J\ddot{\theta}\mathbf{T} + \mathbf{W}_1 + \gamma_2(\dot{\theta}\,|\,\mathbf{x}\mathbf{T} + \mathbf{W}_2) + \mathbf{h}. \tag{2}$$

The quantities $\mathbf{W}_1$ and $\mathbf{W}_2$ are the non-tangential components respectively of the angular inertia and velocity of the rod cross section. The terms involving $\ddot{\theta}$ and $\dot{\theta}$ are the corresponding tangential contributions. The angle $\theta$ is defined so that $\theta' = \omega$ (here, $'$ refers to differentiation with respect to arclength). The quantity $J = \pi a^4/2$ is the massless moment of inertia of a rod cross section about a centered axis normal to the cross section, and $\gamma_2$ is a damping coefficient. The notation $\cdot|\mathbf{x}$ refers to a quantity with respect to fixed $\mathbf{X}$. The second to last term in Eq. (2) is included in order to damp internal motion. However, even without any internal motion of the cross section it is possible for $\theta$ to change due to motion of the base curve $\mathbf{X}$ (see Section 4). This effect is a purely geometrical one and is not subject to any dynamical damping. Thus it is important to damp only the non-geometrical part of $\dot{\theta}$, namely $\dot{\theta}|\mathbf{x}$. The term $\mathbf{h}$ contains any external moments that may be acting on the rod. Dill [23] has described a simplification of (2) due to Kirchhoff in which the terms involving $\mathbf{W}_1$ and $\mathbf{W}_2$ are dropped. This approximation is adopted here. The range

of validity of this assumption as an asymptotic approximation of the full elasticity equations is unclear, although in all the results presented here damping is significant and thus the inertial term $\mathbf{W}_1$ can be expected to be small anyway. A related and in principle closer approximation to full elasticity, sometimes called unshearability, is that the tangent vector $\mathbf{T}$ is always perpendicular to the material cross section. However, this approximation requires a matching of the non-tangential angular acceleration $\mathbf{W}_1/\rho J$ with $\ddot{\mathbf{T}}$, and, as $\mathbf{W}_1$ is expected to be small here, the extra computation does not seem justified.

Equations (1) and (2) are supplemented by the constitutive relation of linear elasticity

$$\mathbf{M} = EI(\kappa - \kappa_0)\mathbf{B} + \mu J(\omega - \omega_0)\mathbf{T}, \tag{3}$$

where $E$ is the *Young's modulus*, $\mu$ is the *torsional rigidity*, and $I = J/2$ is the massless moment of inertia of a rod cross section about a centered axis in the plane of the cross section. $\kappa = |d\mathbf{T}/ds|$ is the curvature of $\mathbf{X}$, and $\omega$ is the twist of a reference ribbon as defined previously. $\mathbf{B}(s, t)$ is the binormal vector defined by the Frenet–Serret equations [24],

$$\begin{aligned} \frac{d}{ds}\mathbf{T} &= \kappa\mathbf{N} \\ \frac{d}{ds}\mathbf{N} &= -\kappa\mathbf{T} + \tau\mathbf{B} \\ \frac{d}{ds}\mathbf{B} &= -\tau\mathbf{N}. \end{aligned} \tag{4}$$

The quantity $\tau$, the torsion, is easily calculated to be the twist of the ribbon $(\mathbf{X}, \mathbf{X} + \mathbf{N})$ (wherever $\mathbf{N}$ is defined and differentiable). For simplicity it will be assumed here until stated otherwise that $\kappa_0 = \omega_0 = 0$. Also note that $EI$ and $\mu J$ are often denoted as, respectively, $A$, the elastic bending coefficient and, $C$, the torsional rigidity coefficient, particularly in the biological literature.

The unit vectors $\mathbf{T}$, $\mathbf{N}$, and $\mathbf{B}$ form an orthonormal triad which is at first glance convenient for rods with circular cross section because of (3). Note, however, that $\mathbf{N}$ and $\mathbf{B}$ are only defined when $\kappa \neq 0$ and, in general, vary discontinuously through points with $\kappa = 0$. Instead, using the ribbon vector $\mathbf{V}$, it is possible to construct a more practical material orthonormal basis $\mathbf{T}$, $\mathbf{V}$, $\mathbf{U} = \mathbf{T} \times \mathbf{V}$, Then (4) are replaced by

$$\begin{aligned} \frac{d}{ds}\mathbf{T} &= \kappa_1\mathbf{V} + \kappa_2\mathbf{U} \\ \frac{d}{ds}\mathbf{V} &= -\kappa_1\mathbf{T} + \omega\mathbf{U} \\ \frac{d}{ds}\mathbf{U} &= -\omega\mathbf{V} - \kappa_2\mathbf{T}, \end{aligned}$$

where $\kappa_1 = \kappa\mathbf{N}\cdot\mathbf{V}$ and $\kappa_2 = \kappa\mathbf{N}\cdot\mathbf{U}$.

The system (1) and (2) will now be scaled as follows. Let $L$ be a characteristic lengthscale of the rod (e.g., total arclength at time 0) and let $T$ be the timescale for a linear torsional wave to traverse this lengthscale. Then $L/T \sim (\mu/\rho)^{1/2}$, the characteristic velocity of linear torsional waves [16]. Define dimensionless variables $L\tilde{s} = s$, $L\tilde{\mathbf{X}} = \mathbf{X}$, $T\tilde{t} = t$, $\rho L^2/T^2\tilde{\mathbf{F}} = \mathbf{F}$, $\rho L^3/T^2\tilde{\mathbf{g}} = \mathbf{g}$, $\rho L^3/T^2\tilde{\mathbf{M}} = \mathbf{M}$, $\rho L^2/T^2\tilde{\mathbf{W}}_1 = \mathbf{W}_1$, $L/T\tilde{\mathbf{W}}_2 = \mathbf{W}_2$, and $\rho L^2/T^2\tilde{\mathbf{h}} = \mathbf{h}$. After dropping the tildes, (1), (2), and (3) become

$$\frac{d^2}{dt^2}\mathbf{X} = \frac{d}{ds}\mathbf{F} - \eta_1\frac{d}{dt}\mathbf{X} + \mathbf{g} \tag{5}$$

$$\frac{d}{ds}\mathbf{M} = \mathbf{F}\times\mathbf{T} + \ddot{\theta}\mathbf{T} + \mathbf{W}_1 + \eta_2(\dot{\theta}|\mathbf{x} + \mathbf{W}_2) + \mathbf{H} \tag{6}$$

$$\mathbf{M} = \Gamma^{-1}\kappa\mathbf{B} + \omega\mathbf{T}. \tag{7}$$

The dimensionless numbers $\Gamma = \mu J/EI = C/A$ and $\eta_i = \gamma_i T/\rho$ measure respectively the relative energetic importance of twist and flexure and the relative time scales of viscosity and inertia. As mentioned above we will set $\mathbf{W}_1 = \mathbf{W}_2 = 0$ throughout.

An additional remark to be made here concerns the relation between $EI$ and $\mu J$. Now $\mu$, the shear modulus, is related to the Young's modulus $E$ by

$$\mu = \frac{E}{2(1+\sigma)}. \tag{8}$$

The constant $\sigma$ is called the *Poisson's ratio*. On physical grounds $\sigma$ lies between 0 and $\frac{1}{2}$ (with $\sigma = \frac{1}{2}$ corresponding to incompressibility). For real physical materials and circular cross sections, then, the ratio $\mu J/EI = \Gamma$ should lie between 1 and $\frac{2}{3}$ (with $\frac{2}{3}$ corresponding to incompressibility). We will use $\Gamma = 1$ throughout.

## 3. TENSION

Equation (5) determines $\ddot{\mathbf{X}}$ in terms of $\mathbf{F}$, $\dot{\mathbf{X}}$, and $\mathbf{g}$, and Eq. (6) and relation (7) determine $\mathbf{F}_\perp \equiv F_N\mathbf{N} + F_B\mathbf{B}$. However, the tension $F_T \equiv \mathbf{F}\cdot\mathbf{T}$ is as yet undetermined. For an extensible filament the tension is proportional to the extension. We wish, however, to consider stiff filaments here; for an incompressible or slightly compressible rod the speeds of nonlinear bending and torsional waves are slower than the extensional wave speed. In order to avoid introducing a short time scale associated with extensional waves we instead enforce inextensibility through the filament tension $F_T$ as will be discussed below. Then the notion of inextensibility will be generalized to allow proscribed extension.

$\mathbf{T}(s, t)$ is a unit vector field for all $t$ and thus $\dot{\mathbf{T}} = \mathbf{\Lambda} \times \mathbf{T}$ for some $\mathbf{\Lambda}(s, t)$ such that $\mathbf{\Lambda}\cdot\mathbf{T} = 0$. Then $\mathbf{T}\cdot\dot{\mathbf{T}} = 0$ and

so $\mathbf{T}\cdot\ddot{\mathbf{T}} = -\dot{\mathbf{T}}\cdot\dot{\mathbf{T}} = -\Lambda^2$. Also, $\mathbf{T}\cdot\ddot{\mathbf{T}} = \mathbf{T}\cdot\ddot{\mathbf{X}}' = \mathbf{T}\cdot(\mathbf{F}'' - \gamma_1\dot{\mathbf{T}}) = \mathbf{T}\cdot\mathbf{F}''$ (by (1)). Writing $\mathbf{F} = F_T\mathbf{T} + \mathbf{F}_\perp$ as above one obtains

$$\mathbf{T}\cdot\frac{d^2}{dt^2}\mathbf{T} = \mathbf{T}\cdot\frac{d^2}{ds^2}\mathbf{F} = \frac{d^2}{ds^2}F_T - \kappa^2 F_T + \mathbf{T}\cdot\frac{d^2}{ds^2}\mathbf{F}_\perp.$$

Thus,

$$\frac{d^2}{ds^2}F_T - \kappa^2 F_T = -\mathbf{T}\cdot\frac{d^2}{ds^2}\mathbf{F}_\perp - \Lambda^2. \tag{9}$$

The quantities on the right-hand side of (9) are known and, together with the appropriate boundary conditions ($F_T(0, t) = F_T(L, t) = 0$ for open rods and periodic for closed rods in the absence of external loading), determine the tension $F_T$.

It is now possible to generalize to the situation of a rod with proscribed extension rate $r(s, t)$. Let $\mathscr{T}$ be a material tangent vector to $\mathbf{X}$ with, for definiteness, $|\mathscr{T}(s, 0)| = 1$. Let $\sigma(s, t)$ be a material parametrization of $\mathbf{X}$, i.e., one that stretches and contracts along with $\mathbf{X}$, such that, for definiteness, $\sigma(s, 0) = s$. Set $ds/d\sigma = A(s, t)$. Then

$$\mathscr{T}(s, t) = A(s, t)\mathbf{T}(s, t) = \frac{d}{d\sigma}\mathbf{X}(s, t).$$

Proceeding as before, set $\dot{\mathscr{T}} = \mathbf{\Lambda}\times\mathscr{T} + r\mathscr{T}$, where $\mathscr{T}\cdot\mathbf{\Lambda} = 0$. Observe that $\mathscr{T}\cdot\dot{\mathscr{T}} = rA^2$ and $\mathscr{T}\cdot\dot{\mathscr{T}} = \mathscr{T}\cdot(\dot{A}\mathbf{T} + A\dot{\mathbf{T}}) = A\dot{A}$, so $\dot{A} = rA$ (with $A(s, 0) = 1$). Also

$$\mathscr{T}\cdot\ddot{\mathscr{T}} = -\dot{\mathscr{T}}\cdot\dot{\mathscr{T}} + \dot{r}A^2 + 2rA\dot{A} = (-\Lambda^2 + \dot{r} + r^2)A^2.$$

Noting that

$$\frac{d^2}{dt^2}\mathscr{T} = \frac{d^2}{dt^2}\frac{\partial}{\partial\sigma}\mathbf{X} = \frac{\partial}{\partial\sigma}\frac{d^2}{dt^2}\mathbf{X} = \frac{\partial}{\partial\sigma}\left(\frac{d}{ds}\mathbf{F} - \gamma_1\frac{d}{dt}\mathbf{X}\right) = A\frac{d^2}{ds^2}\mathbf{F} - A\gamma_1\frac{d}{dt}\mathbf{T}$$

it then follows that $\mathscr{T}\cdot\ddot{\mathscr{T}} = A^2\mathbf{T}\cdot\mathbf{F}''$ and, thus, calculating as before, one obtains

$$\frac{d^2}{ds^2}F_T - \kappa^2 F_T = -\mathbf{T}\cdot\frac{d^2}{ds^2}\mathbf{F}_\perp - \Lambda^2 + \frac{d}{dt}r + r^2. \tag{10}$$

Again the right-hand side of (10) depends only on known quantities and, hence, determines the tension $F_T$ in such a way that arclength is proscribed according to the function $r$.

## 4. TWIST AND WRITHE

An important additional issue involves tracking of the twist evolution in a moving filament. From Eq. (2), if $\mathbf{X}$ is fixed then

$$\frac{d^2\omega}{dt^2} = \frac{\mu}{\rho}\frac{d^2\omega}{ds^2} - \frac{\gamma_2}{\rho J}\frac{d\omega}{dt}, \tag{11}$$

the familar torsional wave equation [16] with dissipation. However, the definition of twist involves the conformation of the base curve $\mathbf{X}(s, t)$. Hence deformations of $\mathbf{X}$ that carry the reference ribbon rigidly may still, and, in fact, in general they do, change the twist $\omega(s, t)$. Note that for a short material section $\Delta_L$ of rod that is stretching (only), $\omega\Delta_L$ is a constant (this is a statement of conservation of twist). Thus $(\omega\dot{\Delta}_L) = 0$ and so

$$\frac{d^2\omega}{dt^2} = -\left(\frac{d^2}{dt^2}\ln\Delta_L\right)\omega - \left(\frac{d}{dt}\ln\Delta_L\right)\frac{d\omega}{dt}.$$

If, for example, $\Delta_L(t) = \Delta_L(0)e^{rt}$ with $r$ a constant, then $\dot{\omega} = -r\omega$ and so constant rate filament stretching without other motion results in a decrease in twist. This is, in fact, intuitively clear. If a length of rod is stretched with no change in total twist then $\omega$, the twist per unit length, must decrease proportionally to the stretching.

Twist can also be changed through rigid motion of the base curve without any arclength deformation. This effect can be illustrated by a simple experiment. Extend your arm horizontally in front of you with wrist bent so that your hand points straight up. Your hand and arm can be thought of as vectors of an untwisted ribbon (with your arm as the base curve). Now rotate your arm 90° down to your waist, then 90° out to the side, and then 90° back to its original position, all without any twisting of the wrist. Note that the head-hand "ribbon" has gained a 90° rotation despite no intrinsic twisting having occurred. This experiment also illustrates the idea of a "geometric phase" occurring upon the circuit of certain classical or quantum systems around a closed path [25].

The equation for the change in $\omega$ under an inextensible

deformation of $\mathbf{X}$ that rigidly moves the reference ribbon is [26] (see also [27, 28])

$$\frac{d}{dt}\omega = \kappa \mathbf{B} \cdot \dot{\mathbf{T}}. \tag{12}$$

Combining these various possibilities one then obtains the twist evolution equations (in non-dimensional form)

$$\begin{aligned}\frac{d^2\omega}{dt^2} - \frac{d^2\omega}{ds^2} = &-\left(\frac{d^2}{dt^2}\ln A\right)\omega - \frac{d}{dt}\ln A \frac{d}{dt}\omega \\ &+ \frac{d}{dt}\left(\kappa \mathbf{B} \cdot \frac{d\mathbf{T}}{dt}\right) - \eta^2 \frac{d\omega}{dt}\bigg|_{\mathbf{X}}\end{aligned} \tag{13}$$

from (11) and (12). The extra ''inertial'' terms in this equation are essential as they provide a coupling between curve motion and twist.

Next we discuss a geometric characterization of closed curves, the *writhing number* (or *writhe*). The writhing number of a curve $\mathbf{X}$ is a measure of its coiling, or *helicity* (see [29]). A number of equivalent definitions of writhe are available (see, e.g., [30]); a computationally straightforward integral formula is

$$Wr(\mathbf{X}) = \frac{1}{4\pi}\int_{[0,L]}\int_{[0,L]} \frac{(\mathbf{T}(s') \times \mathbf{T}(s)) \cdot (\mathbf{X}(s') - \mathbf{X}(s))}{|\mathbf{X}(s') - \mathbf{X}(s)|^3}\, ds'\, ds. \tag{14}$$

Showing that the integrand is 0 in the limit $s \to s'$ is an exercise that will be left to the reader. In particular, any segment $l_i$ of a piecewise linear curve contributes zero self-induced helicity, i.e.,

$$\frac{1}{4\pi}\int_{l_i}\int_{l_i} \frac{(\mathbf{T}(s') \times \mathbf{T}(s)) \cdot (\mathbf{X}(s') - \mathbf{X}(s))}{|\mathbf{X}(s') - \mathbf{X}(s)|^3}\, ds'\, ds = 0$$

and, hence, formula (14) is easily regularizable for discretized curves. It is evident from (14) that $Wr$ is a global characteristic of $\mathbf{X}$ and not a local one.

The writhing number has energetic consequences for the following reason. Defining the *total twist* $Tw$ by

$$Tw(\mathbf{X}) = \frac{1}{2\pi}\oint \omega(\mathbf{X}(s))\, ds,$$

then the quantity

$$Lk(\mathbf{X}) = Tw(\mathbf{X}) + Wr(\mathbf{X}) \tag{15}$$

is a topological invariant and, thus, is constant under crossing-free deformations of the curve $\mathbf{X}$ [31–34] (for the purposes of this paper $Lk$ is the linking number [35] of the curves $\mathbf{X}$ and $\mathbf{X} + \mathbf{V}$). Note that $Lk$ and $Tw$ depend on the choice of reference ribbon but $Wr$ does not. With the choice of notation $Lk(\mathbf{X})$ and $Tw(\mathbf{X})$ the dependence on the ribbon vector $\mathbf{V}$ is suppressed. Also, although the twist $\omega$ depends on the parametrization, the total twist $Tw$ does not. It is easily shown that $Lk(\mathbf{X})$ and $Wr(\mathbf{X})$ jump by $\pm 2$ upon curve crossings and $Tw$ is clearly continuous for all smooth deformations.

Now the energy of a linear elastic rod is

$$E = \text{K.E.} + \frac{1}{2}\int_{[0,L]} (EI(\kappa - \kappa_0)^2 + \mu J(\omega - \omega_0)^2)\, ds, \tag{16}$$

where K.E. is the kinetic energy of the system and at static equilibrium $\omega = \text{const}$ [16], so that $\omega$ and $Tw$ are linearly related. From (15), however, $\Delta Tw = -\Delta Wr$. Hence in closed systems twist can be stored as writhe at the cost of increased curvature and, thus, the writhing number provides a geometric diagnostic of elastic energetics. In particular, writhe provides a measure of the conversion of internal twist to external geometrical structure.

## 5. NUMERICAL SETUP

The curve $\mathbf{X}$ and twist $\omega$ are discretized into a number of points $\mathbf{x}_i$ and twist at these points $\omega_i$ which evolve according to second-order centered difference schemes for (5), (7), (13), and the non-tangential part of (6). Time evolution is done using a Runge–Kutta integrator. A contact force $\mathbf{\Psi}$ is added to Eq. (5). The contact force takes the form of a stiff inverse power law ($\mathbf{\Psi} \sim r^{-10}$) with a ''charge'' density 1 concentrated at the discretization points. (Here charge density does not refer to a physical electrostatic charge but one following an $r^{-10}$ law,) $\mathbf{\Psi}$ is scaled so that the filament radius $a$ is approximately two to three discretization lengths. The requirement $a/L \ll 1$ is a necessary one for numerical stability and convergence. The stiff power law is chosen in order to approximate a sharp boundary contact force. The issue of sensitivity of results to choice of contact force is not investigated here. The function $\mathbf{h}$ in Eq. (6) is set to zero. The tension is determined in a manner to be described below.

A very important feature of any numerical scheme for filament simulations is tension. Tension is necessary to keep the points $\mathbf{x}_i$ from flying apart. This can be accomplished by using springs to tie adjacent points together (e.g., [7]). However, for stiff filaments like the ones considered here, resolving the spring time scale may necessitate overly small time steps and/or implicit integrators. To avoid such remedies we instead derived in Section 3 a

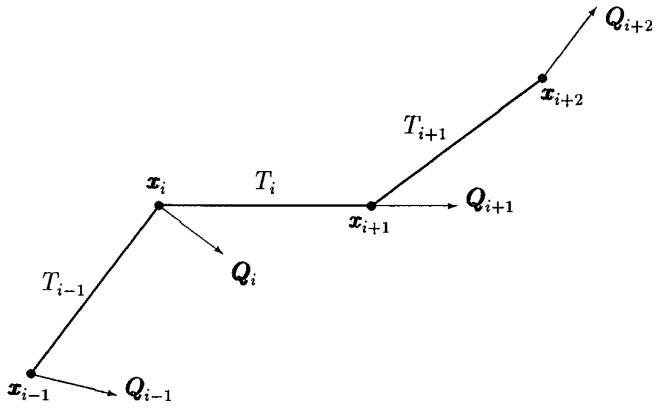


**FIG. 2.** Discrete forces on a section of the chain $\{\mathbf{x}_i\}$.

method to simulate inextensible filaments and filaments of proscribed extension. A tension $F_T$ which satisfies (10) will enforce a proscribed arclength. However, a naive discretization of (10) may fail because truncation errors tend to set off numerical instabilities. It is instead desirable here to derive a discretization that works to round-off error. We can also use this opportunity to provide an alternative, direct derivation by calculating the balance of forces on the piecewise linear chain discretization of the smooth rod. This approach also suggests a way of generalization to higher dimension. Figure 2 illustrates a short segment of the chain encompassing the points $\mathbf{x}_{i-1}$ through $\mathbf{x}_{i+2}$. The $\mathbf{Q}_i$ are the forces on the points $\mathbf{x}_i$ calculated from discretizations of Eqs. (5) and (6), except not including $F_T\mathbf{T}$. For simplicity set the distance between each pair of points to be $h$ and assume that $h$ is constant in time. Let $T_i$ be the tension on the chain segment between $\mathbf{x}_i$ and $\mathbf{x}_{i+1}$. Then the point $\mathbf{x}_i$ feels a tension force $h^{-1}(T_i\mathbf{t}_i - T_{i-1}\mathbf{t}_{i-1})$, where $\mathbf{t}_i$ is the unit vector pointing from $\mathbf{x}_i$ to $\mathbf{x}_{i+1}$.

We now consider the forces necessary to keep $\mathbf{x}_i$ and $\mathbf{x}_{i+1}$ at a constant distance. First, if $\mathbf{t}_i \times (\dot{\mathbf{x}}_{i+1} - \dot{\mathbf{x}}_i) \neq 0$ then a centrifugal force of magnitude $h^{-1}|\mathbf{t}_i \times (\dot{\mathbf{x}}_{i+1} - \dot{\mathbf{x}}_i)|^2 = h\dot{\mathbf{t}}_i^2$ is necessary to keep $\mathbf{x}_i$ and $\mathbf{x}_{i+1}$ from flying apart. Additionally it is necessary to balance the $\mathbf{t}_i$ component of $\mathbf{Q}_{i+1} - \mathbf{Q}_i$. To satisfy these two requirements it is necessary that the tension solves

$$h^{-1}\mathbf{t}_i \cdot [(T_{i+1}\mathbf{t}_{i+1} - T_i\mathbf{t}_i) - (T_i\mathbf{t}_i - T_{i-1}\mathbf{t}_{i-1})] = -\mathbf{t}_i \cdot (\mathbf{Q}_{i+1} - \mathbf{Q}_i) - h(\dot{\mathbf{t}}_i)^2.$$

Discretizing the relation $\kappa = |d\mathbf{T}/ds|$ by $\kappa_i = h^{-1}|\mathbf{t}_i - \mathbf{t}_{i-1}|$ and noting that $\mathbf{t}_i \cdot \mathbf{t}_{i-1} = 1 - (h^2\kappa_i^2/2)$, one obtains

$$\frac{1}{h}(T_{i+1} - 2T_i + T_{i-1}) - \frac{\kappa_{i+1}^2 h}{2} T_{i+1} - \frac{\kappa_i^2 h}{2} T_{i-1} = -\mathbf{t}_i \cdot (\mathbf{Q}_{i+1} - \mathbf{Q}_i) - h(\dot{\mathbf{t}}_i)^2, \tag{17}$$

the desired second-order discretization consistent with (9). Equation (17) is a tridiagonal system for open filaments and is tridiagonal plus two off-diagonal elements for closed systems. Either way, inversion is a straightforward $O(n)$ operation [36]. The generalization of (17) to account for proscribed extension is

$$\frac{1}{h}(T_{i+1} - 2T_i + T_{i-1}) - \frac{\kappa_{i+1}^2 h}{2} T_{i+1} - \frac{\kappa_i^2 h}{2} T_{i-1} = -\mathbf{t}_i \cdot (\mathbf{Q}_{i+1} - \mathbf{Q}_i) - h(\dot{\mathbf{t}}_i)^2 + h\dot{r} + hr^2. \tag{18}$$

Use of (17) or (18) to calculate tension still introduces instabilities over relatively long times due to errors introduced by time discretization. These errors can be removed by eliminating spurious tangential velocities. The requirement $\dot{\mathbf{T}} \cdot \mathbf{T} = 0$ for local arclength conservation can be easily seen to imply

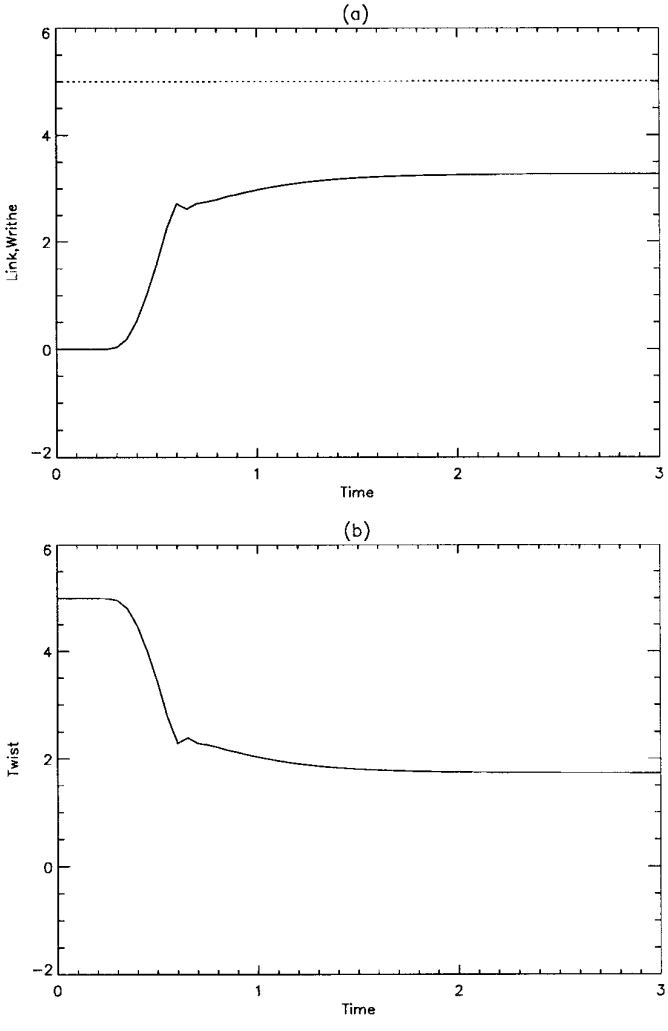


**FIG. 3.** Evolution of *Tw* and *Wr* for the clover-leaf example: (a) *Lk* (dashed curve) and *Wr* (solid curve) versus time; (b) *Tw* versus time.

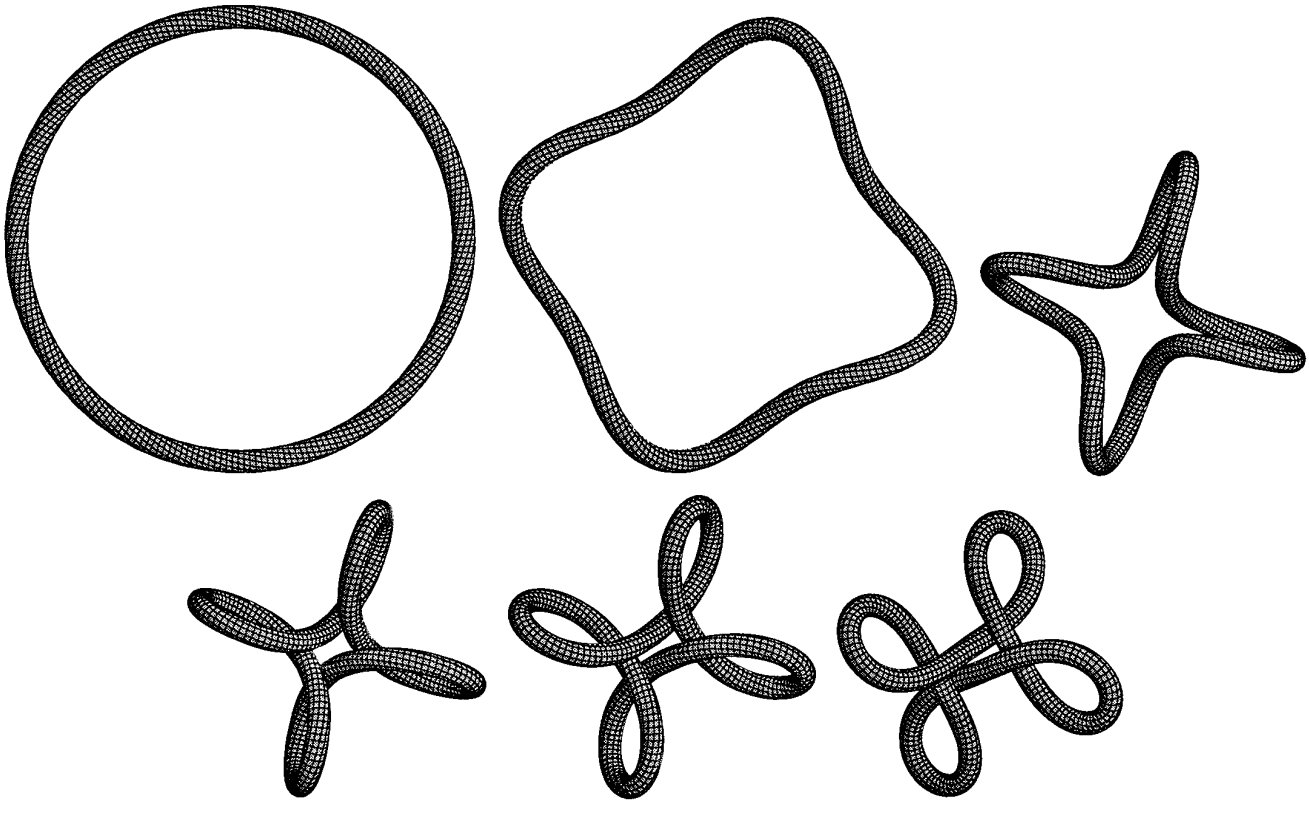

**FIG. 4.** Approach to equilibrium "clover" conformation. First row: $t = 0$, $t = 0.40$, $t = 0.55$. Second row: $t = 0.75$, $t = 0.95$, $t = 3.0$.

$$\frac{d}{ds} q_{\mathbf{T}} = \kappa q_{\mathbf{N}}, \tag{19}$$

where $q_{\mathbf{T}}$ and $q_{\mathbf{N}}$ are the tangential and normal components respectively of $\dot{\mathbf{X}}$. In principle (19) should be satisfied automatically due to the presence of the tension force satisfying Eq. (17). However, as mentioned, time discretization introduces small errors that result in (19) not being exactly satisfied and can cause instability if unchecked. This problem is fixed by adding a tangential velocity so that (19) is satisfied to round-off precision. The additional velocity, which can be calculated using a similar procedure to the one presented above, is very small and results in no noticeable change in diagnostic statistics. This procedure generalizes easily to the proscribed extension case.

In Section 7 we will be considering an open rod with constant arclength growth rate $r(s, t) = r_0$ at each point resulting in exponential growth of total arclength. In order to maintain accuracy, a regriding occurs after each arclength doubling time by inserting a new discretization point between each pair of old discretization points using first-order interpolation. This simple interpolation scheme conserves total twist (both locally and globally).

The main error checking method was a convergence study using decreasing discretization lengths. Other diagnostics included conservation of various quantities including the linking number (15) for closed rods. An additional check comes from the verification of the Zajac instability criterion for closed filaments (to be described in the next section), providing support for both the numerical results and the Zajac and Benham analyses.

## 6. INSTABILITY AND STABILITY OF CLOSED RODS

An inextensible rod closed into a circle with uniformly distributed twist is easily seen to be in equilibrium. However, this equilibrium is known to be unstable for sufficiently large twist. The critical total twist $\Omega$ has been calculated [10, 37, 5] to be $\Omega = \sqrt{3}(EI/\mu J) = \sqrt{3}\Gamma^{-1}$. For the special case $\Gamma = 0$ (i.e., no contribution to the twist energy) it is in fact known that, in the absence of contact forces, the circle is the only stable equilibrium [38]. In general, however, the question of identification of stable equilibria is open, with or without contract forces. Much work has been done on generating equilibrium configurations using the static rod equations, usually without contact forces, but apparently little is known about the stability of these configurations (see, e.g., [39]).

Beginning with [4, 40], elastic rod and related systems have now been used in DNA modelling for a number of

**FIG. 5.** Approach to equilibrium "plectonemic" conformation. First row: $t = 0$, $t = 0.35$, $t = 0.45$. Second row: $t = 0.55$, $t = 0.75$, $t = 0.95$. Third row: $t = 1.25$, $t = 1.55$, $t = 3.50$.

years (see [41] for a recent review). Typically in such models it is assumed that the twist $\omega - \omega_0$ is constant along the rod (the equilibrium state) and then using (15) the term $\oint (\omega - \omega_0)^2 \, ds$ in (16) can be replaced (up to a constant) by $(Lk - Wr)^2$. This simplification allows one to drop $\omega$ altogether and base all computation only on the geometry of the curve $\mathbf{X}$. The new energy functional can then be minimized using, for example, a Monte Carlo-type descent method [42]. More involved simulations (Langevin dynamics) using descent for the same energy functional with the addition of viscosity and random forcing terms (to model a finite temperature Brownian environment) have achieved some success in modelling circular DNA dynamics [43]. All the numerics presented in this section use dissipation but no forcing and thus we observe monotonic energy dissipation and no dynamic fluctuations. The simulations presented here do allow for non-uniform twist so, in principle, one could add forcing to the present model in an attempt to improve on the studies mentioned above. Of course, DNA is not a classical elastic rod and it is not clear that an improved approximation of an elastic rod would lead to improved modelling of DNA dynamics. This issue of the validity of modelling DNA as an elastic rod is a topic of current interest [44, 45]. Nevertheless it seems possible that the assumption of uniform twist may be at least quantitatively significant and a better representation of twist might be useful. In some applications allowance for twist dynamics is essential (see Section 7). We present here a few simulations using the more "realistic" model (although without dynamic fluctuations).

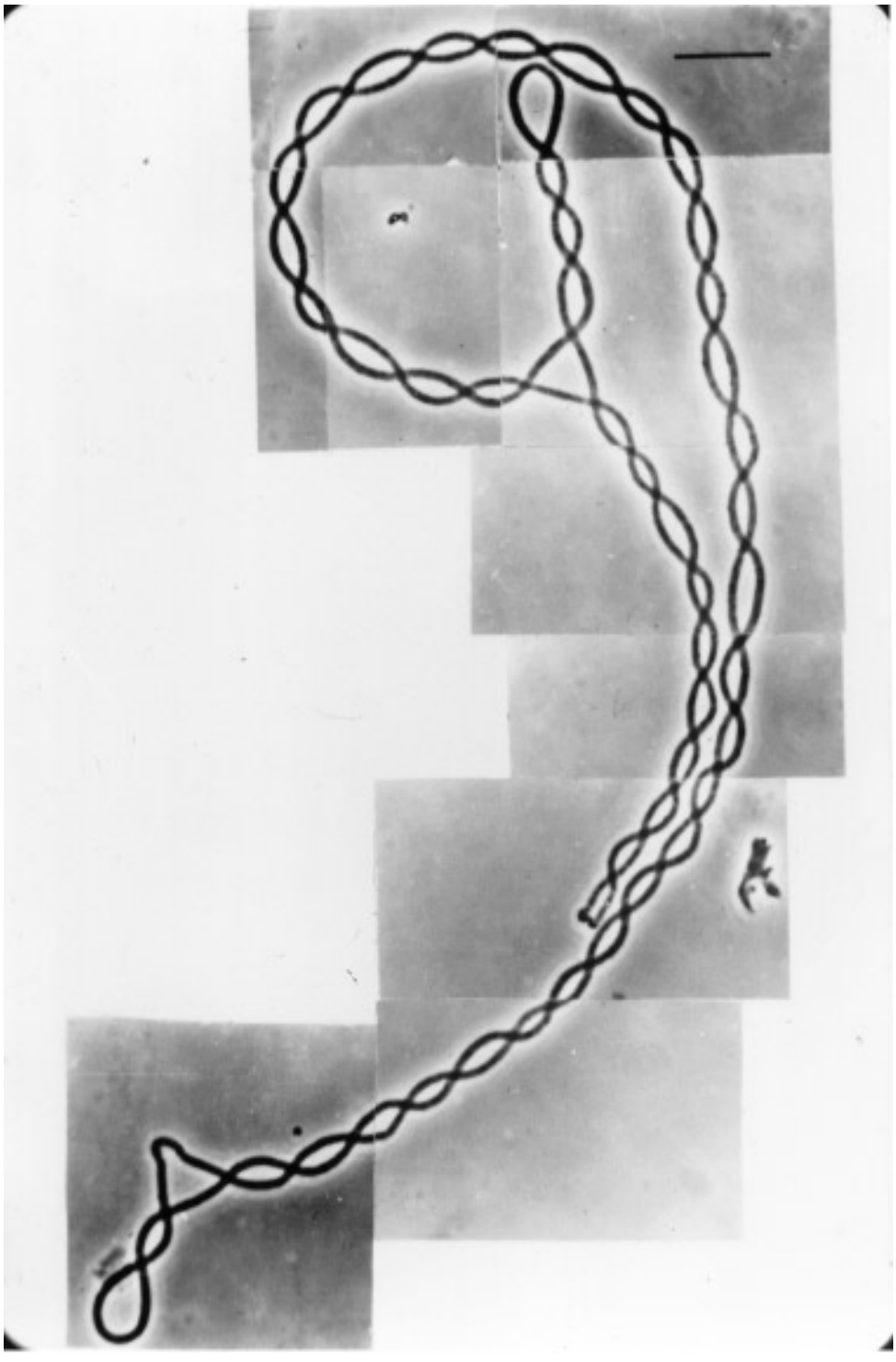

**FIG. 6.** Photograph of a filament of *bacillus subtilis* at an advanced stage of self-assembly. Each visible "strand" is actually composed of many pieces of the bacterial filament.

In the circular (unstable) equilibrium conformation, the rod has twist and no writhe (see Section 4). As instability occurs, twist energy is decreased by the conversion of twist to writhe. Hence the dynamical process that is observed might be called a *writhing instability.* In this section the dynamics of the writhing instability (also known as the supercoiling instability) are simulated and some resulting stable equilibrium configurations are presented. Disallowing rod passage, $Lk = Tw + Wr$ holds with $Lk$ constant, and, thus, the instability is eventually halted because the

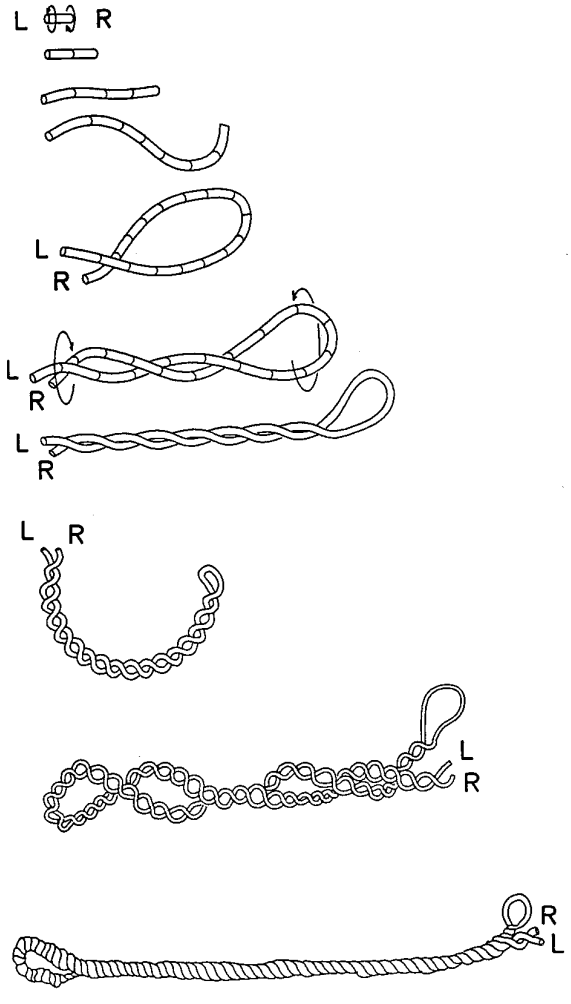


**FIG. 7.** Schematic of the writhing instability of *bacillus subtilis* (originally published in [47].

rod is unable to ''unwind'' by passing through itself. This fact allows the possibility for the rod to become stuck in a local minimum. In Fig. 3 the behaviors of $Lk$, $Wr$, and $Tw$ are shown for certain initial conditions (the ''clover'' conditions, see below). $Lk$ is constant as expected and $Tw$ and $Wr$ evolve continuously but are approximately constant after contact occurs. A sequence of snapshots of the dynamics of approach to equilibrium for two examples ($\Gamma = 1, r_0 = \frac{1}{2}$) are shown in Figs. 4 and 5. In both examples the initial conditions are chosen to be a circular conformation with $Tw = 5$. The four-leaf clover in the final frame of Fig. 4 is the eventual equilibrium when the initial twist is distributed uniformly with a small localized perturbation. The final frame of Fig. 5 illustrates the eventual equilibrium conformation for exactly the same parameters and initial conditions as the first example, except that the initial twist includes an order one non-localized perturbation from uniformity, in particular, $\omega(s, 0) = 2\pi(Tw/L)(1 + 0.5 \sin(2\pi s/L))$. The equilibrium of Fig. 5 is sometimes called the plectonemic conformation and is familar to DNA studies (e.g., [41]). It is stressed that the final conformations of Figs. 4 and 5 are distinct obtainable local energy minima of unknotted closed rods with identical linking number. For the particular case shown here the plectonemic structure has roughly $\frac{2}{3}$ the energy of the clover structure. Dynamic fluctuations would, of course, favor the lower energy structure, but at sufficiently low temperatures both might exist. In fact clover-like structures are observable in Langevin dynamics simulations [46].

## 7. DYNAMICS OF OPEN RODS

The results presented in this section are motivated by a desire to model behavior of filaments of the bacteria *bacillus subtilis* [21]. Individual cells of this bacteria grow as an extending cylinder with diameter of approximately 0.8 $\mu$m and maximum length approximately 3 to 4 $\mu$m prior to cell division. As growth occurs, cell wall structures composed of the polymer peptidoglycan apparently induce twist in the cell walls [22]. Although these polymers seem to have an important role in the cell structure, their geometry is largely unknown. Another important feature of the growth process for this bacterial strain is that after division, the cells fail to separate. Thus the bacteria cells form an exponentially growing filament doubling in length over a time of the order of 70 min. At a certain point the extending filament becomes unstable, eventually contacting itself and forming a closed structure which quickly winds up plectonemically into a double helical conformation. In this fashion twist converts into writhe. Next the resulting double helical structure grows exponentially, becomes unstable, and eventually forms a quadruple-stranded plectonemic structure, and so on. Eventually thick strands of interwound bacteria are produced (Fig. 6). This striking behavior is an example of a biological self-assembly process. A schematic of the writhing sequence is shown in Fig. 7. The filament instability resembles that commonly observed in twisted rubber bands. There are some significant differences, however; for example, unlike a twisted rubber band, the ends of the bacteria filament are free. Furthermore the supercoiling that occurs in a rubber band has the opposite handedness to the twist, whereas in the bacteria filament system the handedness is the same.

It is proposed here that the bacteria filament and its self-assembly process can be modelled by a dynamical Kirchhoff viscoelastic rod with contact forces and filament growth. The aim of modelling the bacteria is somewhat different than that of DNA modelling. Rather than obtaining quantitative information we wish to gain qualitative information about the structure of the bacterial cell walls by demonstrating that a few simple assumptions about the *bacillus subtilis* system (and, in particular, the cell walls)

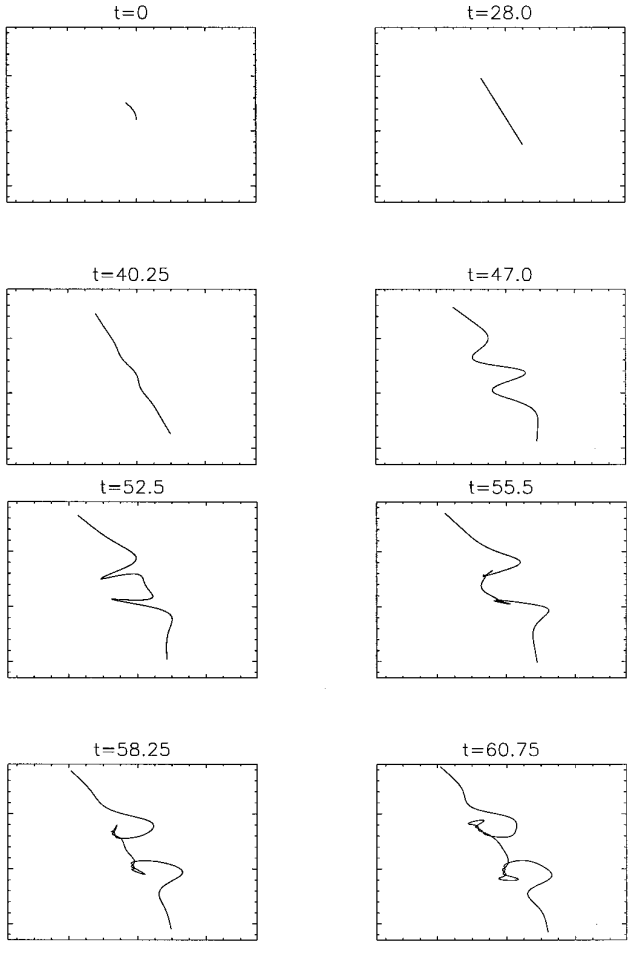


**FIG. 8.** Writhing instability in an exponentially growing filament. First row: $t = 0$, $t = 28.0$. Second row: $t = 40.25$, $t = 47.0$. Third row: $t = 52.5$, $t = 55.5$. Fourth row: $t = 58.25$, $t = 60.75$.

can explain the complicated behavior observed under the microscope. Thus through simulations of a basic model, the initial aim at least is to qualitatively reproduce the bacteria filament behavior.

The assumptions to be made are as follows. First, the chain of bacteria cells in a medium can be modelled as a linear viscoelastic rod as described in the previous sections of this paper. Second, at all points of the bacteria chain, the cells are growing at the same (constant in space and time) rate. This assumption could be relaxed to the assumption that each cell is growing and dividing on average at a certain rate. Third, backbone polymers in the cell wall prefer energetically to maintain a helical structure with a (constant in space and time) twist rate $\omega_0$. Lastly the effects of Brownian motion and fluid dynamics are neglected (except for viscous drag).

Assumptions 2 and 3 affect the Kirchhoff rod model as follows. Assumption 3 just says that in the constitutive law (3), $\omega_0$ is a non-zero constant (a linear restoring force is implicitly assumed). To satisfy assumption 2 the exponential growth rate of the bacteria is enforced by adding a growth term $r^2$ to the tension equation as described in Section 3. The filament is not inextensible but instead changes length in a proscribed non-dynamic way. In non-dimensional form $r^2 = (T/T_{gr})^2$, roughly the square of the ratio of the wave time scale to the length doubling time scale. A more subtle consequence of assumption 2 comes from its effect on twist evolution. As can be noted from Eq. (13) (with $\ln A = rt$) the presence of stretching results in a decrease in twist from the equilibrium value $\omega_0$ thus effectively introducing a twist deficit, or a twist opposite in handedness to the equilibrium twist. When the twist deficit becomes sufficiently large, a writhing (or supercoiling) instability occurs.

A representative sequence of simulation filament conformations is shown in Fig. 8. In this simulation $\Gamma = 1$, $\eta_1 = \eta_2 = 20$, $r = 10^{-2}$, and $\omega_0 = 8$. The simulation extends over four filament doubling times (about 70 non-dimensional time units) starting from initial conditions consisting of a slightly bent filament of length $\pi/2$ non-dimensional units with initial twist $\omega = \omega_0$. The filament initially straightens in the viscous medium but eventually becomes unstable, deforming into a helix-like shape and then forming two plectonemic side-branches at about time 50–55. In Fig. 9 the total twist $\int \omega\, ds$ is plotted versus time. The change in rate of gain of twist at the time of plectoneme formation is seen clearly. This writhing instability allows more twist to be quickly introduced to the filament, temporarily relieving the twist deficit.

A plot of $\omega(s, t)$ is illuminating. The filament starts with initial conditions $\omega(s, 0) = \omega_0$. As time elapses, filament stretching causes $\omega$ to decrease towards 0. The ends of the filament are able to maintain $\omega \sim \omega_0$, and twist originating from the open ends of the filament is able to replenish $\omega$

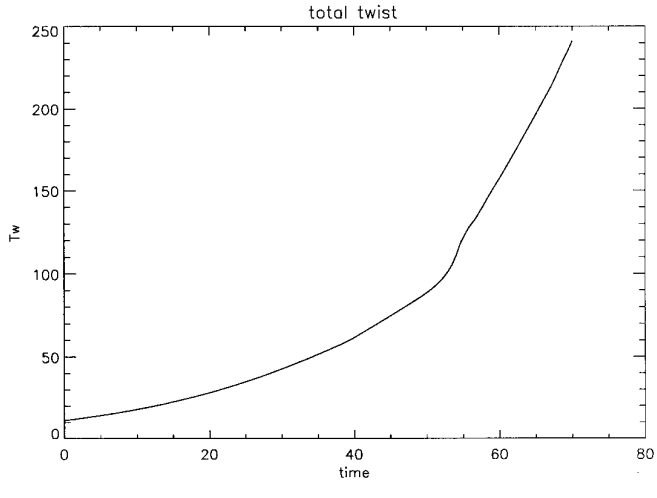


**FIG. 9.** Total twist *Tw* versus time for the filament shown in Fig. 8.

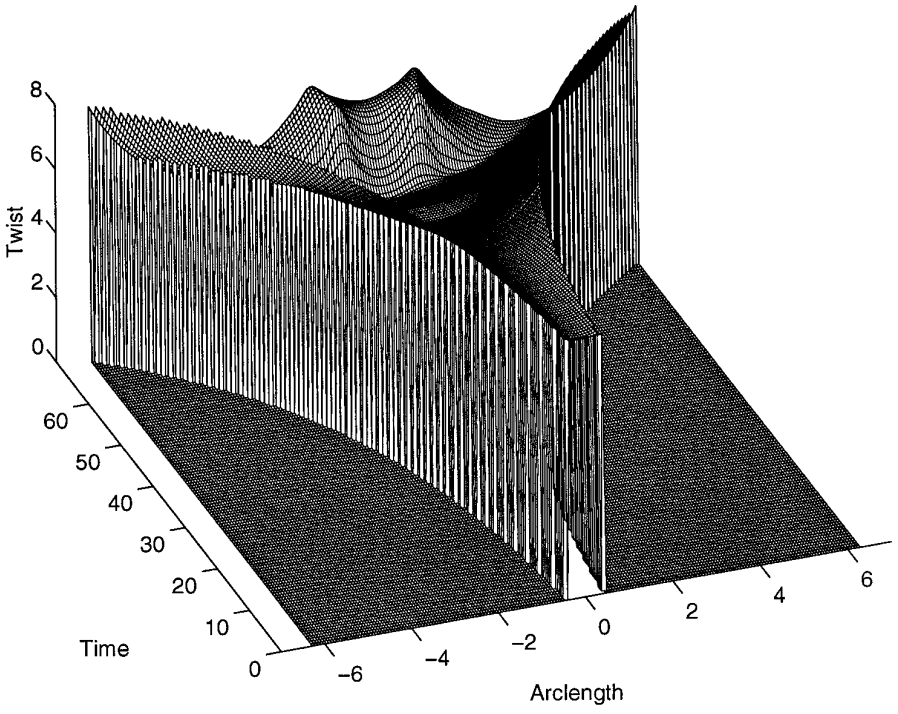


**FIG. 10.** The surface $\omega(s, t)$ for the filament shown in Fig. 8 is a twist as a function of arclength and time.

in the filament interior for a time. Eventually, however, the filament becomes too long for twist to penetrate to the central part of the filament quickly enough (the twist wave speed is constant) and so $\omega$ decreases rapidly there. This results in an increase in the twist potential energy density $\Gamma(\omega - \omega_0)^2$ and leads to a supercoiling instability to relieve the twist energy and reduce the twist deficit.

## 8. CONCLUSIONS

A practical working algorithm for the dynamical evolution of an elastic Kirchhoff rod with proscribed extension has been presented. The algorithm is based on the idea of modelling a thin filament as a space curve with scalar twist (or framing). The algorithm includes contact forces and dissipation both from an external viscous medium and from an internal damping. Proscribed extensibility or inextensibility is enforced through a special choice for the tension. This tension although globally determined is still easily calculable. Twist evolution is decomposed into effects of internal twist dynamics, rod motion kinematics, and rod extension. (Some additional details can be found in [48].)

The principle computational innovations introduced here are the use of detailed dynamics of twist and the enforcement of proscribed rod extensibility. The presented algorithm has been employed to consider two problems of biological interest, namely, the existence of distinct obtainable stable equilibria of closed rods with contact forces starting from similar initial conditions and the possibility for interesting behavior in open rods. This last result is of special importance for understanding the non-trivial behavior of *bacillus subtilis*, and it is expected that the present algorithm will successfully model many aspects of the bacteria's behavior qualitatively. It is also hoped that the simulations of writhing instabilities in closed rods presented here will stimulate further analysis of these instabilities. At present there is only partial understanding [49] of even the linearized problem.

## ACKNOWLEDGMENTS

The author would like to give special thanks to M. Tabor, A. Rao, and A. Goriely for their considerable assistance. In addition the author benefited from conversations with N. Mendelson, comments from C. Benham, and criticisms of J. Maddocks. This work was supported by DOE Grant DE-FG03-93-ER25174 and an NSF post-doctoral fellowship.

## REFERENCES

1. H. Hasimoto, *J. Fluid Mech.* **51,** 477 (1972).
2. J. P. Keener, *J. Fluid Mech.* **211,** (1990).
3. J. Langer and R. Perline, *J. Nonlinear Sci.* **1,** 71 (1991).
4. F. B. Fuller, *Proc. Nat. Acad. Sci. U.S.A.* **75,** 3557 (1978).
5. C. J. Benham, *Phys. Rev. A* **39,** 2582 (1989).
6. H. Tsuru and M. Wadati, *Biopolymers* **25,** 2083 (1986).

7. T. Schlick and W. K. Olson, *Science* **257,** 1110 (1992).
8. J. J. Tyson and S. H. Strogatz, *Int. J. Bifur. Chaos* **1,** 723 (1991).
9. J. F. Keener and J. J. Tyson, *SIAM Rev.* **34,** 1 (1992).
10. E. E. Zajac, *J. Appl. Mech.* **29,** 136 (1962).
11. H. C. Spruit, *Astron. Astrophys.* **98,** 155 (1981).
12. S. D'Silva and A. R. Choudhuri, *Astron. Astrophys.* **272,** 621 (1993).
13. G. Kirchhoff, *Mechanik* **28** (1876).
14. A. Clebsch, *Theorie der Elasticitat Fester Korper* (Teubner, Leipzig, 1862).
15. A. E. H. Love, *A Treaty on the Mathematical Theory of Elasticity,* 4th ed. (Cambridge Univ. Press, 1927; Dover, New York).
16. L. D. Landau and E. M. Lifschitz, *Theory of Elasticity* (Pergamon, Oxford, 1959).
17. B. D. Coleman and E. H. Dill, *J. Acoust. Soc. Am.* **91,** 2663 (1992).
18. D. J. Dichmann, J. H. Maddocks, and R. L. Pego, preprint.
19. J. C. Simo and L. Vu-Quoc, *Appl. Mech. Eng.* **58,** 79 (1986).
20. J. H. Maddocks *et al.*, personal communication, 1995.
21. N. H. Mendelson, *Sci. Progress Oxford* **74,** 425 (1990).
22. J. J. Thwaites and N. H. Mendelson, *Adv. Microbiol. Physiol.* **32,** 174 (1991).
23. E. H. Dill, *Arch. Hist. Exact Sci.* **44,** 2 (1992).
24. M. P. Do Carmo, *Differential Geometry of Curves and Surfaces* (Prentice-Hall, Englewood Cliffs, New Jersey, (1976).
25. M. V. Berry and J. H. Hannay, *J. Phys. A: Math. Gen.* **21,** L325 (1988).
26. I. Klapper and M. Tabor, *J. Phys. A: Math. Gen.* **27,** 4919 (1994).
27. J. H. White, *Proc. Symp. Pure Math.* **27,** 429 (1975).
28. J. Yunger, preprint.
29. H. K. Moffatt and R. L. Ricca, *Proc. R. Soc. A* **439,** 411 (1992).
30. J. Aldinger, I. Klapper, and M. Tabor, *J. Knot Theory Ramifications* **4,** 343 (1995).
31. G. Calugareanu, *Czechoslavak Math. J.* **11,** 588 (1961).
32. W. F. Pohl, *J. Math. Mech.* **17,** 975 (1968).
33. J. H. White, *Am. J. Math.* **91,** 693 (1969).
34. F. B. Fuller, *Proc. Nat. Acad. Sci. U.S.A.* **68,** 815 (1971).
35. D. Rolfsen, *Knots and Links* (Publish or Perish, Berkeley, 1976).
36. W. H. Press, B. P. Flannery, S. A. Teukolsky, and W. T. Vetterling, *Numerical Recipes* (Cambridge Univ. Press, Cambridge, 1986).
37. M. LeBret, *Biopolymers* **18,** 1709 (1979).
38. J. Langer and D. A. Singer, *Topology* **24,** 75 (1985).
39. Y. Shi and J. E. Hearst, *J. Chem. Phys.* **101,** 5186 (1994).
40. C. J. Benham, *Proc. Nat. Acad. Sci. U.S.A.* **74,** 2397 (1977).
41. T. Schlick, *Curr. Opin. Struct. Biol.* **5,** 245 (1995).
42. A. V. Vologodskii and N. R. Cozzarelli, *Annu. Rev. Biophys. Biomol. Struct.* **23,** 609 (1994).
43. T. Schlick and W. K. Olson, *Biophys. J.* **67,** 2146 (1994).
44. W. R. Bauer and C. J. Benham, *J. Mol. Biol.* **238,** 1184 (1993).
45. J. F. Marko and E. D. Siggia, *Macromolecules* **27,** 981 (1994).
46. G. Ramachandran and T. Schlick, Beyond optimization: Simulating the dynamics of supercoiled DNA by a macroscopic model, to appear, in *DIMACS Series in Discrete Mathematics and Theoretical Computer Science,* edited by P. Pardalos, D. Shalloway, and G. Xue (Am. Math. Soc., Providence, Rhode Island, 1995).
47. N. H. Mendelson and J. J. Thwaites, *Mat. Res. Soc. Symp. Proc.* **174,** 171 (1990).
48. M. Tabor and I. Klapper, Dynamics of twist and writhe and the modeling of bacterial fibers, to appear, in *Mathematical Approaches to Biomolecular Structure and Dynamics,* IMA **82,** edited by J. P. Mesirov, K. Schulten, and D. W. Sumners, (Springer-Verlag, New York, 1995).
49. F. Tanaka and H. Takahashi, *J. Chem. Phys.* **83,** 6017 (1985).